

AlN piezoelectric materials for wireless communication thin film components

Ju-hyung Kim^{a,b}, Si-Hyung Lee^a, Jin-Ho Ahn^b and Jeon-Kook Lee^{*,a}

^aThin Film Technology Research Center, KIST, Seoul 136-791, Korea

^bDepartment of Materials Science and Engineering, Hanyang University, Seoul 133-791, Korea

A Bragg reflector type FBAR using AlN piezoelectric with quarter wavelength thickness has been fabricated, where the Bragg reflector was composed of W-SiO₂ pairs. By numerical simulation, considering actual acoustic losses of each layer, an analysis of the frequency response of the resonator has been made and this could be explained using an equivalent circuit with parasitic elements. The Effective electromechanical coupling constant (K_{eff}^2) and the Quality factor (Q_s), figures of merit of the resonator, were about 1.1% and 307, respectively.

Key words: Bragg reflector, FBAR, AlN.

Introduction

With the recent development of wireless communication, there has been an increased demand for microwave filters monolithically integrable with semiconductor devices. Film Bulk Acoustic wave Resonator (FBAR) based microwave filters is an economically attractive alternative to dielectric filters and Surface Acoustic Wave (SAW) filters because they have advantages of small size, low cost by mass production and compatibility with semiconductor processes [1].

The basic structure of a FBAR consists of a piezoelectric layer sandwiched between two electrodes on the substrate. In the FBAR structure, an acoustic wave should be confined to the piezoelectric layer. Such acoustic isolation from the substrate can be realized by means of an air gap or Bragg reflector. In case of a Bragg reflector, this is composed of several pairs of alternating quarter wavelength layers with high acoustic impedance contrast. Such a set may transform the input acoustic impedance of the substrate to a very low or to a very high value as alternating sequence.

For acoustic isolation, if the input acoustic impedance of the substrate transforms to a very low value, a piezoelectric layer with a half wavelength thickness should be used to form half wavelength standing waves in the piezoelectric layer. By contrast, if the input acoustic impedance of the substrate transforms to a very high value, a piezoelectric layer with a quarter wavelength thickness should be used to form quarter wavelength standing waves [2-4].

Much research has reported on Bragg reflector type

FBARs (BR FBAR) [5-7]. However, BR FBARs with a piezoelectric layer of a quarter wavelength thickness have not been reported about. In this study, we observed the frequency response of BR FBAR with a piezoelectric layer of a quarter wavelength thickness. The structure was designed for resonance at about 2.4 GHz and a Bragg reflector of six layers was used. We also numerically analyzed the frequency response taking into account acoustic losses of each layer in the fabricated structure.

Experimental

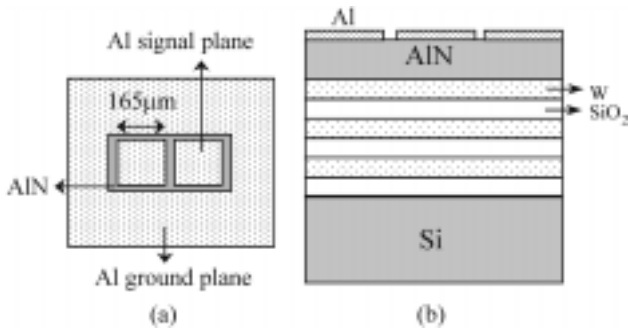
The resonator was fabricated on an (100) oriented Si substrate. AlN and Al were chosen as a piezoelectric layer and an electrode, respectively. W was chosen as a high acoustic impedance material and SiO₂ was chosen as a low acoustic impedance material for the Bragg reflector, respectively.

To make six Bragg reflector layers, W and SiO₂ of quarter wavelength thickness were *in situ* deposited on the Si substrate by rf magnetron sputtering. AlN and Al were deposited on the Bragg reflector layers by rf magnetron sputtering. Deposition conditions of each layer were summarized in Table 1. 0.1 μm thick Al electrode was patterned and wet etched by developer (AZ 300 MIF). Active area of 165² μm² was formed. Figure 1 shows a schematic structure of the resonator. The film thickness and microstructure were observed using a field emission scanning electron microscope (Hitachi). The surface roughness was measured using an atomic force microscope (Park Scientific Instrument). The S₁₁ parameter was measured using a network analyzer (HP 8510C and HP 8753D) and Pico probe (GGB Inc.). The probe and the network analyzer were calibrated using a calibration substrate for the load, short and open standard.

*Corresponding author:
Tel : +82-2-958-5563
Fax: +82-2-958-6951
E-mail: jkleemc@kist.re.kr

Table 1. Deposition conditions of each layer in the structure of Bragg reflector FBAR

	AlN	Al	W	SiO ₂
Target material/size	Al/2"	Al/2"	W/2"	SiO ₂ /2"
Base pressure	$<5 \times 10^{-5}$ Pa	$<5 \times 10^{-5}$ Pa	$<5 \times 10^{-4}$ Pa	$<5 \times 10^{-4}$ Pa
Working pressure	0.133 Pa	0.133 Pa	0.4 Pa	0.267 Pa
Gas flow rate (sccm)	N ₂ =20	Ar=10	Ar=30	Ar/O ₂ =36/4
Rf power	300W	75W	40W	150W
Distance between target and substrate	6 cm	6 cm	6 cm	6 cm
Substrate temperature	RT	RT	200°C	RT

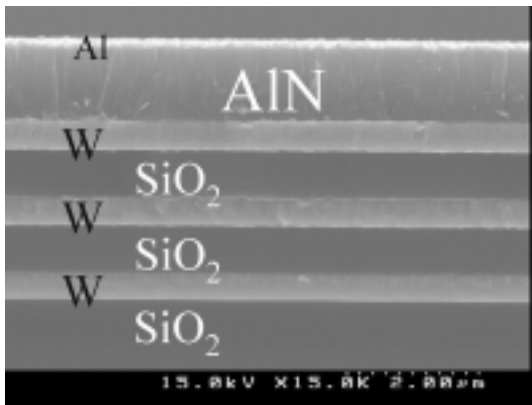
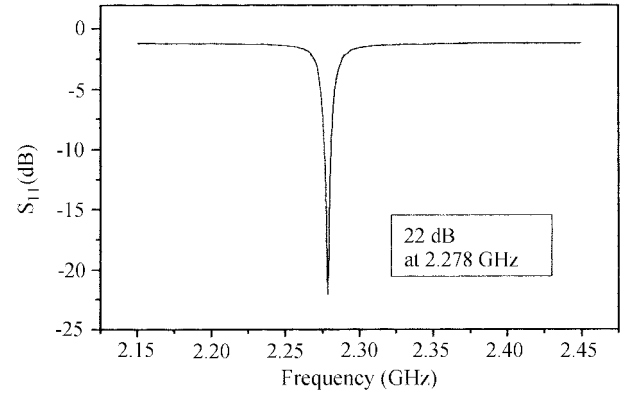
**Fig. 1.** Schematic representation of the Bragg reflector FBAR structure; (a) Top view and (b) Cross-sectional view.

Result and Discussion

Figure 2 shows the cross sectional microstructure of the fabricated resonator. The AlN piezoelectric layer shows a dense columnar structure. In the Bragg reflector, the W layer also had a columnar structure and the SiO₂ layer was almost an amorphous.

The measured narrow band return loss (S_{11}) of the resonator is shown in Fig. 3. The magnitude of return loss (S_{11}) was about 22 dB at 2.278 GHz. From the S_{11} data, we could obtain the input electrical impedance ($Z_{in,e}$) using the following equation.

$$Z_{in,e} = Z_0 \left(\frac{1+S_{11}}{1-S_{11}} \right) \quad (1)$$

**Fig. 2.** Cross sectional SEM micrograph of a Bragg reflector FBAR fabricated on a Si (100) substrate.**Fig. 3.** The measured return loss (S_{11}) of Bragg reflector FBAR.

where, Z_0 is 50Ω . We also simulated an input electrical impedance in the narrow band using transmission line theory in order to compare this with the measured one. In the Bragg reflector, the acoustic impedance transforming properties of layer are described by the expression for the input acoustic impedance of the layer placed on the substrate. The input acoustic impedance of all the layers is calculated by employing the following equation n times successively [2].

$$Z_{in}^{(i)} = Z_c^i \frac{Z_{in}^{(i-1)} \cos b_i l_i + i Z_c^i \sin b_i l_i}{Z_c^i \cos b_i l_i + Z_{in}^{(i-1)} \sin b_i l_i} \quad (2)$$

where, $Z_c^{(i)}$ is the material acoustic impedance of the i th layer, $Z_{in}^{(i-1)}$ is the input acoustic impedance of the $(i-1)$ th layer, b_i are the complex wave vectors for the i th layer, l_i are their thickness, $Z_{in}^{(0)} = Z_s$ (the material acoustic impedance of the substrate), and $i = 0, 1, \dots, n$.

The Bragg reflector with 6 layers was designed to transform the input acoustic impedance of the substrate (Z_s) to a very high value ($Z_{in}^{(6)}$) at the interface with the piezoelectric layer. Then the input electrical impedance of the resonator is calculated using the following equation [4].

$$Z_{in,e} = \frac{1}{i\omega C_0} \left(1 + \frac{K^2}{1 + K^2} \frac{1}{bl(Z_0 + Z_t Z_b)} \frac{i(Z_t + Z_b)Z_0 \sin bl - 2Z_0^2(1 - \cos bl)}{\sin bl - i(Z_t + Z_b)Z_0 \cos bl} \right) \quad (3)$$

where, Z_t is the input acoustic impedance of the top

Table 2. Attenuation constant (α) of each layer in the structure of Bragg reflector FBAR used in simulation

Attenuation constant (α) at 1 GHz	
AlN	5 (dB/ μ s)
Al	13.63 (dB/ μ s)
W	0.14 (dB/ μ s)
SiO ₂	43.86 (dB/ μ s)

electrode and Z_b is the input acoustic impedance at the top layer of the Bragg reflector on the substrate ($Z_{in}^{(6)}$). k is the electro-mechanical coupling constant, C_0 is the capacitance, Z_0 is the material acoustic impedance, b is the complex wave vectors, l is the thickness of the piezoelectric material.

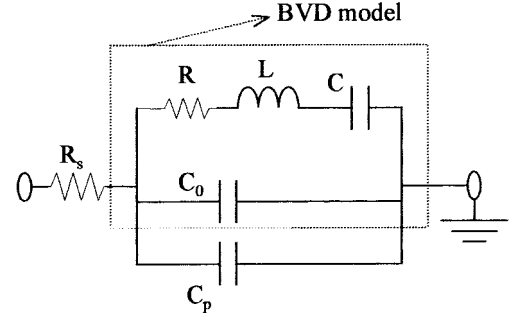
In order to consider acoustic losses in the fabricated structure, we added an attenuation value to the wave vector of each layer in equation (4). The attenuation constants used in simulation are listed in Table 2. In addition, we considered the acoustic loss in the piezoelectric layer by scattering of acoustic waves due to the surface roughness. So we calculated the attenuation value from the surface roughness using the following equation used by Mansfeld [8-10].

$$\alpha_{rough}(dB/\mu s) = -4.34 \cdot \frac{10^{-6}}{2d} \cdot V_s [q^2 \eta_1^2 + q^2 \eta_2^2] \cdot 4\pi \quad (4)$$

where, d is the thickness, V_s is the wave velocity, q is the phase constant, η_1 and η_2 are the mean roughness

Table 3. Attenuation constant (α) by surface roughness and RMS value in the AlN piezoelectric layer. (η_1 is on the Al electrode, η_2 is on the top layer of Bragg reflector.)

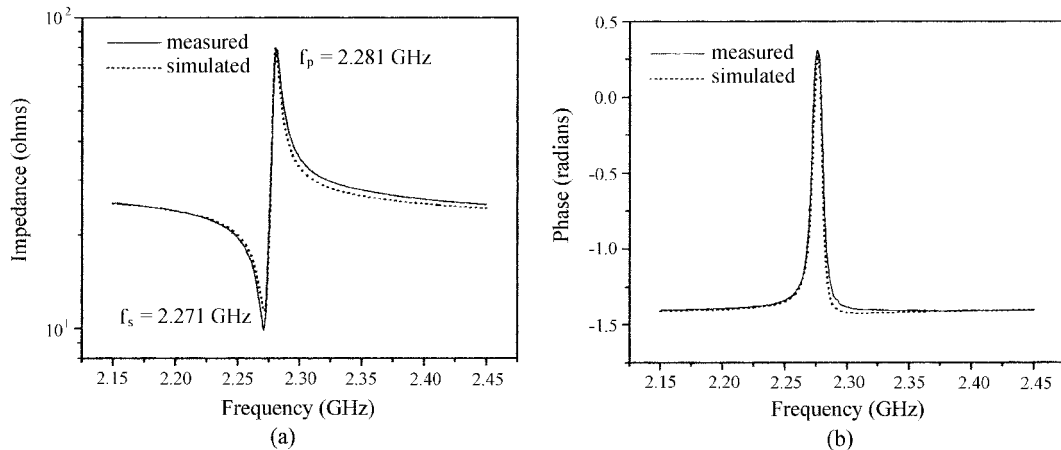
RMS value of surface roughness (nm)	Attenuation constant (dB/ μ s)
$\eta_1 = 12.6$	16.68
$\eta_2 = 6.25$	


Fig. 4. An equivalent circuit with parasitic elements used in the simulation of the Bragg reflector FBAR, where R_s is the series resistance and C_p is the parasitic capacitance.

amplitude in the top electrode and the top layer of the Bragg reflector on the substrate, respectively. The surface roughness and attenuation values are listed in Table 3. The roughness scan was performed over $5^2 \mu\text{m}^2$ area and the surface roughness was similar over many positions on the Al electrode and the top layer of Bragg reflector.

However, the input electrical impedance ($Z_{in,e}$) simulated through such a procedure was different from the measured one. Hence we modeled an equivalent circuit with some parasitic elements on the basis of the Butterworth Van-Dyke (BVD) model as shown in Fig. 4. In this model, we could infer parasitic element values from the wide band input electrical impedance response in the frequency range without resonance. The inferred parasitic series resistance and the parallel capacitance were 4Ω and 0.7 pF , respectively.

The simulated input electrical impedance and the phase response were very similar to the measured input electrical impedance and the phase response when we used this model with these parasitic values. Figure 5 shows the input electrical impedance ($Z_{in,e}$) and phase response with a frequency, which were measured and simulated, respectively. It is thought that the parasitic capacitance in the electrode interconnects and the sheet


Fig. 5. Simulated and measured frequency response of the Bragg reflector type FBAR; (a) Input electrical impedance and (b) Phase of input electrical impedance.

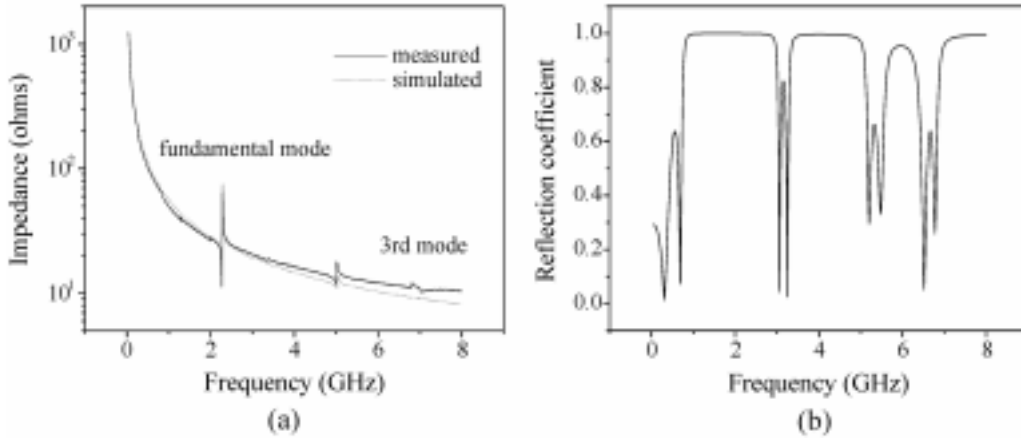


Fig. 6. Wide band frequency response of the Bragg reflector FBAR; (a) Simulated and measured input electrical impedance and (b) Simulated reflection coefficient.

resistance of the electrode had some effect on the input electrical impedance and the phase response of the resonator.

Additionally, we investigated the wide band input electrical impedance response to confirm a narrow band simulation. Figure 6 shows the measured and simulated input electrical impedance ($Z_{in,e}$) and the simulated reflection coefficient in the wide band. The wide band simulated impedance response was similar to the measured one for the most part. A small difference was shown in the high frequency region. However, this is thought to be negligible because the difference of impedance was only a few ohm.

The wide band response shows fundamental and third mode as a general description of an ideal resonator model. Further, the parasitic mode near 5 GHz appeared in both measured and simulated impedance responses. It is thought that the parasitic mode occurred due to the poor acoustic isolation considering the reflection coefficient in this frequency ranges as shown in Fig. 6(b).

From the measured frequency response of the resonator, we calculated the Effective electromechanical coupling constant (K_{eff}^2) and the Quality factor ($Q_{s/p}$) using the following equations.

$$K_{eff}^2 = \frac{\frac{\pi f_s}{2 f_p}}{\tan\left(\frac{\pi f_s}{2 f_p}\right)} \approx \left(\frac{\pi}{2}\right)^2 \frac{f_p - f_s}{f_p} \quad (5)$$

$$Q_{s/p} = \frac{f_x}{2} \left. \frac{dZ_{in}}{df} \right|_{f_x=f_{s/p}} \quad (6)$$

The calculated and values were about 1.1% and 307, respectively.

Conclusions

In the Bragg reflector type FBAR, we could infer parasitic effects by numerical simulation considering the acoustic losses of each layer in the experimentally obtained structure. The inferred parasitic series resistance and parallel capacitance were 4Ω and 0.7 pF, respectively. The Effective electromechanical coupling constant (K_{eff}^2) and the Quality factor ($Q_{s/p}$) were about 1.1% and 307, respectively.

Acknowledgments

The Authors thank Prof. Mansfeld for helpful discussions.

References

1. S.V. Krishnaswamy, and J. Rosenbaum, *Microwaves & RF*, Sep. (1991) 127-135.
2. G.D. Mansfeld, S.G. Alekseev, and I.M. Kotelyanskii, 1998 IEEE Ultrasonics Symposium, Oct. 5 10 (1998) 963-967.
3. G.D. Mansfeld, and S.G. Alekseev, *Ultrasonics, Ferroelectrics, And frequency of control society*, Oct. 5 8 (1999) 69-72.
4. G.D. Mansfeld, *Tech. Phys. Lett.* 23[10] Oct. (1997) 750-752.
5. M.-A. Dubois, P. Muralt, and H. Matsumoto, 1998 IEEE Ultrasonics Symposium, Oct. 5 10 (1998) 909-912.
6. G.V. Tsarenkov, 1999 IEEE Ultrasonic Symposium (1999) 939-942.
7. M.-A. Dubois, and P. Muralt, 1999 IEEE Ultrasonics Symposium (1999) 907-910.
8. V.V. Kosachev, Y.N. Lokhov, *Sol. State Phys. (Sov)* 31 (1989) 105-113.
9. S.N. Ivanov, and E.N. Khazanov, *Radiotechnics and Electronics (Sov)* 2 (1981) 402-408.
10. G.D. Mansfeld, 1994 IEEE Ultrasonics Symposium (1994) 655-658.